Applied Surface Science Advances 18 (2023) 100479

Contents lists available at ScienceDirect

Applied Surface Science Advances

journal homepage: www.sciencedirect.com/journal/applied-surface-science-advances

Influence of pre-treatments on adhesion, barrier and mechanical properties of epoxy coatings: A comparison between steel, AA7075 and AA2024

A. Trentin [a,d,*], R. Samiee [a], A.H. Pakseresht [a], A. Duran [b], Y. Castro [b], D. Galusek [a,c]

[a] Centre for Functional and Surface Functionalized Glass, Alexander Dubček University of Trenčín, Študentská 2, 911 50 Trenčín, Slovakia
[b] Instituto de Cerámica y Vidrio (ICV-CSIC), Campus de Cantoblanco, 28049 Madrid, Spain
[c] Joint Glass Centre of the IIC SAS, TnUAD and FChFT STU, 91150 Trenčín, Slovakia
[d] VTT Technical Research Centre of Finland Ltd., Materials Performance, Kemistintie 3, FI-02044 Espoo, Finland

ARTICLE INFO

Keywords:
Epoxy coatings
DGEBA
Steel
Aluminum
Sol-gel
Bonding mechanisms

ABSTRACT

In this work five independent pre-treatments – mechanical polishing, alkaline and acid etching, sol-gel primer, and anodizing – were applied on mild steel and aluminum (AA7075 and AA2024) substrates before the deposition of epoxy coatings. The results demonstrate that efficient adhesion can be achieved by simple methodologies and widely available chemicals as an alternative to toxic conversion layers or highly energetic processes. All the treatments provided higher adhesion (up to 75%, 61% and 14% on AA7075, AA2024 and steel, respectively) and better anti-corrosion performance (increase of impedance values at low frequency up to four orders of magnitude) than the polished reference. The anodizing of aluminum alloys yielded good anti-corrosion performance, but slightly lower mechanical properties compared to sol-gel primer and alkaline etching. The hydroxyls density was found to play a major role in strong adhesion prevailing over surface roughness, contact area, oxide thickness and hydrophobicity. Despite the efficient performance of hydrogen bonds from acid and alkaline etching on aluminum, these connections do not yield sufficiently stable bonds that make an impermeable barrier of epoxy coatings on steel. Covalent bonds (Me-O-Si) represent the key to achieve a significant improvement in mechanical and chemical resistance against the ingress of water and polymer chain relaxation. This makes the sol-gel primer a simple, economical, and environmentally alternative towards efficient bonding at a molecular level.

Introduction

Epoxy-based coatings are extensively employed materials for corrosion protection. One of the most commonly used epoxy resins to produce coatings and adhesives is the petroleum-based diglycidyl ether of bisphenol A (DGEBA). DGEBA stands out as an important material in anti-corrosion applications due to its capacity to generate a robust, durable, and chemically resistant material [1,2]. Epoxies are a 100% resin product chemically cured with a polyamide hardener, which makes them more durable than acrylic coatings [3] and stiffer than polyurethane coatings [1], resulting in stronger adhesion but slightly inferior aesthetic performance, depending on the application [3]. Nonetheless, loss of adhesion represents one of the most common triggers of blistering, pitting, and crevice corrosion of polymer coatings. When epoxy coatings, e.g., DGEBA, coat metals, they chemically bond to the oxide layer through functional structural groups. The adhesion of DGEBA polymer chains to steel and aluminum oxides is a complex phenomenon that depends on chemical or physical bonds, functional chemical groups, surface roughness and surface-free energy [4,5], making the pre-treatment stage a key approach for ensuring strong adhesion.

The enhancement of polymer-metal bonding is typically based on surface topography (mechanical surface modification), the presence of functional chemical groups, and surface-free energy. The current surface pre-treatment concept varies according to the nature of the metal, desired performance, material application, environment, standards and regulations. Several common methods have been standardized by various industries to achieve strong adhesion and corrosion resistance (Figure S1) [6–8]. The procedures, including surface cleaning and coating application, usually include:

(i) Surface cleaning using solvents, alkaline cleaning agents or detergents.

* Corresponding author.
E-mail address: andressa.trentin@vtt.fi (A. Trentin).

https://doi.org/10.1016/j.apsadv.2023.100479
Received 24 July 2023; Received in revised form 3 October 2023; Accepted 16 October 2023
Available online 21 October 2023

(ii) Chemical etching using acidic or alkaline solutions, or mechanical etching by sanding or abrasive blasting.
(iii) Deoxidizing of aluminum alloys with acid or alkaline solutions and passivation of steel alloys through the application of a protective layer, e.g., corrosion inhibitors or conversion coatings.
(iv) Conversion coating of aluminum is usually performed with solutions containing chromates, phosphates, molybdite, zirconate, anodizing, among others.
(v) Rinse and dry followed by the epoxy coating application by spraying, dipping or brushing.

Mechanical etching such as polishing comprises an abrasive method that aims to increase the contact area with the polymer chains [9]. Even though it is a simple and widely employed method, its applicability is limited for large metallic components on an industrial scale, as it is a labor-intensive and slow process [10]. It has been reported that good adhesion can also be achieved on smooth surfaces with functional groups through acid or alkaline etching [4,6,8]. Hydrogen bonds have been identified as the most important factor contributing to the adhesion between aluminum oxide and epoxy resins by connecting available hydroxyl groups from the metal surface to the resin [4,11]. An interesting way of promoting hydrogen bonds is by adding functional chemical groups that promote acid-base interactions between an interfacial donor and acceptor of an electron pair. However, concentrated solutions lead to the appearance of grooves on the surface that can result in mechanical modification instead of chemical modification, favouring the application of diluted solutions instead [10].

Anodizing is a common electrochemical surface treatment for the application of conversion coatings. This increases surface roughness through the creation of pores and channels that promote a higher contact area with the coating but the high consumption of energy and sluggish processes have driven the development of plasma electrolytic oxidation (PEO) [12], UV/ozone radiation, atmospheric pressure plasma [9], among others. Mechanical theory suggests that interlocking at a macroscopic level controls adhesion under these conditions and sees the interface as a polymer-substrate composite where the coating fills cavities, pores, or rough features [4].

Despite being well established, most of the methods described above include toxic and restricted substances, e.g., chromate conversion coatings, urging the development of green, easy, and affordable solutions. The application of silanes on aluminum substrates has shown the ability to provide functional groups for the subsequent formation of Si-O-Al covalent bonds, which in turn present excellent adhesion properties [13,14]. This is because chemical bonds (ionic or covalent) between the metal oxide and the polymer are known to provide the strongest and most stable connections [4,6,15]. The use of coupling agents has been reported as an efficient strategy to effectively improve surface adhesion by covalent bonds. Organosilanes, for example, can form metallosiloxane bonds across the oxide/polymer interface [4,13], making them a promising alternative to promote the adhesion of polymer coatings at a molecular level.

Van der Waals forces should also be considered during metal processing and coating design since they form between any two molecules in contact [4]. These interactions account for the forces between permanent and induced dipoles, and despite their fragile nature (compared to chemical bonding), they contribute to bonding. Fig. 1 depicts a scheme of the main adhesion theories, summarized into four groups: Van der Waals forces, chemical bonds, acid-base interactions and mechanical interlocking.

Although strong bonding contributes significantly to the performance of coatings [4,5,16], the type of metal oxide and polymer nature are also important, resulting in a great variety of results [17]. In addition, a good adhesion of epoxy coatings may not always guarantee long-term corrosion protection, as polymers physically and chemically age with time. These variables make it complex to predict bonding mechanisms and barrier properties during coatings design. Although

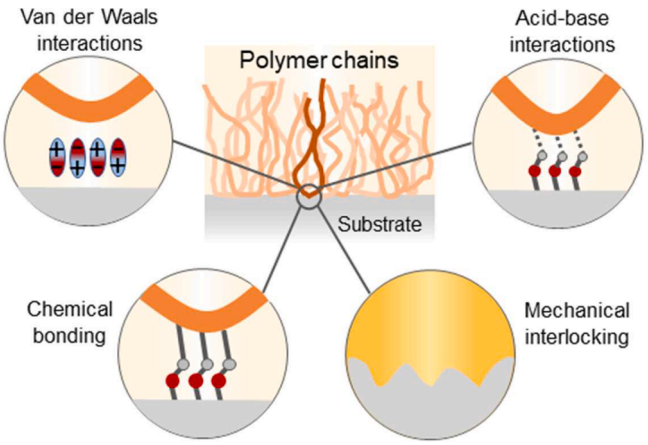

Fig. 1. Representative scheme of adhesion theories between polymer coatings and metal substrates [4,16].

several studies have been dedicated to the understanding of how pre-treatments and surface morphology affect the bonding of epoxy coatings to metal oxides [5,14,16,18–21], a comprehensive/comparative study that considers how they affect the bonding and barrier properties of DGEBA coatings on mild steel, AA7075 and AA2024 has not been, to the best of our knowledge, reported. In addition, a deeper understanding of adhesion mechanisms related to different pre-treatments seems to be reported in very few studies for either aluminum or steel [5,6,14,16,18–22], creating an important literature gap.

Here, we aim to understand the dependence between the chemical nature of DGEBA and the type of substrate/metal oxide using a systematic and comparative methodology. This study applies five independent pre-treatments (polishing, mild alkaline and acid etching, sol-gel and anodizing) on carbon steel, AA7075 and AA2024 substrates, in which DGEBA coatings are deposited by dip-coating. Through surface, mechanical, and electrochemical tests, we demonstrate the role of different pre-treatments in the adhesion and barrier properties of epoxy coatings by correlating them with mechanisms.

Methodology

Pre-treatments

Flat steel and aluminum substrates (2 × 4 × 0.3 cm) were polished using #1000 and #2000 abrasive papers and rinsed with isopropanol before different pre-treatments were applied. Apart from acid, alkaline, anodization, and sol-gel pre-treatments, a reference sample was prepared without any further treatment. For acid etching, a 0.01 M HCl (Centralchem, CAS number: 7647–01–0) solution was prepared (pH 2), and the steel and aluminum coupons were immersed for 10 min at room temperature. For the alkaline pre-treatment, the samples were immersed in a 10^{-3} M KOH (Centralchem, CAS number: 1310–58–3) solution (pH 11.5) for 10 min at 60 °C. The preparation method for the silane layer used in this work was reported elsewhere [23] and consists of mixing 12.24 mL of tetraethyl orthosilicate (TEOS, Merck, CAS number: 78–10–4) with 8.52 mL of ethanol (Merck, CAS number: 64–17–5) and 5.19 mL of an HNO_3 acidified solution, pH 1 (Sigma Aldrich, CAS number: 7697–37–2). The solution was stirred for 1 h at room temperature (RT), and the resulting sol was deposited on the substrates by dip-coating at a withdrawal rate of 30 cm/min and dried at RT.

Anodizing is a process where the substrate is subjected to an anodic current to convert the metal on the surface to an oxide. Depending on the metal, this may form an adherent, corrosion-resistant surface layer, and it is usually carried out on aluminum, titanium, and magnesium. However, this process is useless for steel due to the formation of rust.

The parameters for anodizing aluminum alloys were selected according to the work of Sulka et al. [24]. A 0.3 M oxalic acid (Sigma Aldrich, CAS number: 144–62–7) solution was prepared, and the anodic porous alumina layer was formed by applying a constant voltage of 30 V for 1 hour at RT, using a Pt wire 1 mm thick (20 cm length) as the counter electrode at a distance of 3 cm from the working electrode.

Synthesis of DGEBA solution, coating deposition and curing

A commercial 2-component (2 K) epoxy coating composed of bisphenol A diglycidyl ether (DGEBA, Sigma Aldrich, CAS number: 1675–54–3) was prepared by mixing 18.7 g of DGEBA with 1.3 g of Triethylenetetramine (TETA, Sigma Aldrich, CAS number: 112–24–3) as a curing agent (6.5% vol.), using 20 mL of acetone (Centralchem. CAS number: 67–64–1) as solvent [25]. The solution was left to react for 1 hour at room temperature, and the sol was applied to all pre-treated substrates by dip-coating: all samples were immersed three times (one-minute immersion followed by one minute of drying at room temperature). Next, all samples were dried at 60 °C for 24 h and cured at 160 °C to ensure solvent evaporation and complete polymerization of the coatings. The samples were labelled according to the pre-treatment applied prior to the deposition of DGEBA coatings, namely, reference, acid, alkaline, sol-gel and anodized (only on aluminum), where reference corresponds to the polished surface. Table 1 summarizes the procedures employed in the different pre-treatments of steel, AA7075, and AA2024, correlating them to the previously discussed adhesion hypothesis.

Characterization of the neat surfaces and epoxy-coated specimens

A key approach to understanding the connection between epoxy coatings and metals consists of combining surface, chemical and morphological analysis with mechanical, adhesion and electrochemical testing of coated metal substrates. In this work, the thickness and morphology of the DGEBA-based coatings were obtained from cross-sectional images using a Scanning electron microscopy (SEM) JEOL JSM7600. Before the analysis, the samples were cut and embedded into a conductive resin, polished with alumina (1 μm) and coated with gold to avoid charging and drifting. The images were recorded using an acceleration voltage of 5 kV. The chemical composition and opening of the epoxy ring in the presence of amine (hardener) was verified by a PerkinElmer Spectrum™ 3 spectrometer in the attenuated total reflection module (ATR-FTIR), with a resolution of 4 cm^{-1}, 64 scans and a range of 4000 to 400 cm^{-1}.

An Atomic force microscope (AFM) CERVANTES, NANOTEC Electronic, was employed to obtain information on the roughness of neat substrates after different pre-treatments. The root-mean-square (R_{RMS}) roughness of uncoated AA2024, AA7075 and steel samples was determined as an average from three AFM topography maps of a 5 μm^2 area using the Gwyddion v. 2.62 open source software). Water contact angle measurements were performed to determine the hydrophilic/hydrophobic character of the uncoated metal substrates using Easy drop standard 'Drop Shape Analysis System' Kruss DSA 100 equipment under ambient laboratory conditions. Three measurements were performed on each sample and the average of the results is presented.

Information on the adhesion of the epoxy coatings was obtained using an Elcometer 510 Automatic Pull-off Adhesion Gauge. Aluminum dollies were fixed to the coated specimens using an epoxy 2-component Araldite glue after a slight abrasion of the surface by SiC sandpaper (#600) to improve the fixation. The glued dollies were dried and cured for 3 h at 100 °C prior to the measurements to determine dry and wet adhesion (after 30 days of immersion in seawater during electrochemical tests). The instrument gauge applied a gradually increasing tensile force at a rate of 0.8 MPa/s until the coating was detached from the substrate, and the critical force of coating removal was recorded.

The corrosion barrier properties of the epoxy coatings on differently pre-treated AA7075, AA2024 and steel substrates were studied by immersing the samples in a 3.5% NaCl solution for one month. Electrochemical impedance spectroscopy (EIS) measurements were performed weekly to compare the corrosion protection efficiency of the coatings using a Gamry Potentiostat Reference 600. The coated substrates served as the working electrode in an electrochemical cell along with a saturated calomel electrode (SCE) as the reference and a platinum wire as the counter electrode. The measurements were carried out at room temperature, 10 points per decade, an amplitude of 10 mV(rms), and a frequency ranging from 5 mHz to 1 MHz. The impedance data obtained was fitted with the software Zview® (Scribner Associates, Southern Pines, NC, USA) using electrical equivalent circuits (EEC).

Finally, the mechanical properties of the coatings were investigated by micro scratch tests (performed in triplicate) using an Indenter scratch tester CETR APEX Series. A spherical-conical diamond tip with a 200 μm radius was used at an increasing load (1–10 N) on a 3 mm track at a speed of 9 N/min. The tracks were analysed by optical microscopy to determine the average critical load for coatings failure.

Table 1
Procedures and bonding hypothesis for the five pre-treatments employed on steel, AA7075, AA2024 specimens before deposition of DGEBA-based coatings.

Pre-treatment	Conditions	Substrates	Bonding hypothesis	Ref.
Reference	Polishing with #1000 and #2000 SiC abrasive papers*	Steel AA7075 AA2024	Physical interactions (Van der Waals forces), hydrogen bonds and mechanical interlocking to a minor extent	[4–6, 8]
Alkaline	Immersion in KOH 10^{-3} M for 10 min @ 60 °C	Steel AA7075 AA2024	Physical interactions (Van der Waals forces) and hydrogen bonds	[4–6, 8,16]
Acid	Immersion in HCl 0.01 M for 10 min @ RT	Steel AA7075 AA2024	Physical interactions (Van der Waals forces) and hydrogen bonds	[4–6, 8,16, 26]
Sol-gel	Dipping in sol-gel (TEOS, ethanol, H_2O/HNO_3) @ RT	Steel AA7075 AA2024	Physical interactions (Van der Waals forces) and covalent bonds (mostly)	[4–6, 8,18, 19]
Anodized	Application of 30 V in 0.3 M oxalic acid solution for 60 min @ RT	AA7075 AA2024	Physical interactions (Van der Waals forces), hydrogen bonds and mechanical interlocking (mostly)	[4–6, 8,16, 27]

* Procedure employed before all treatments.

Results and discussion

Composition, morphology, wettability and thickness of neat and coated substrates

During the polymerization of epoxies, the curing agent (an aliphatic amine) reacts with the oxirane rings yielding tertiary amines [28]. The optimal ratio (epoxy/amines) is reached when stoichiometric amounts of epoxy groups and active hydrogens from primary amines react. After synthesizing and drying the DGEBA coatings, the surface was evaluated by FTIR operated in the ATR mode (Fig. 2). The vibrational bands that are characteristic of functional groups of DGEBA and TETA were identified according to the literature. The aliphatic groups of DGEBA (C—H of CH_2, CH_3 and aromatic CH) are shown in spectra with vibrations in the range 2975–2870 cm^{-1}; also, the aromatic ring (inset in Fig. 2) presents stretching vibrations at 1608 cm^{-1} and the C—C bonds are detected at 1508 cm^{-1} [29,30]. Evidence for the opening of the epoxy ring is found in the stretching vibrations at 1037 cm^{-1} [31], and at 825 cm^{-1} due to the 1,4-aromatic ring substitution (-C=C<). In addition, the suppression of the band at 915 cm^{-1} (C—O-C bond of the oxirane ring)

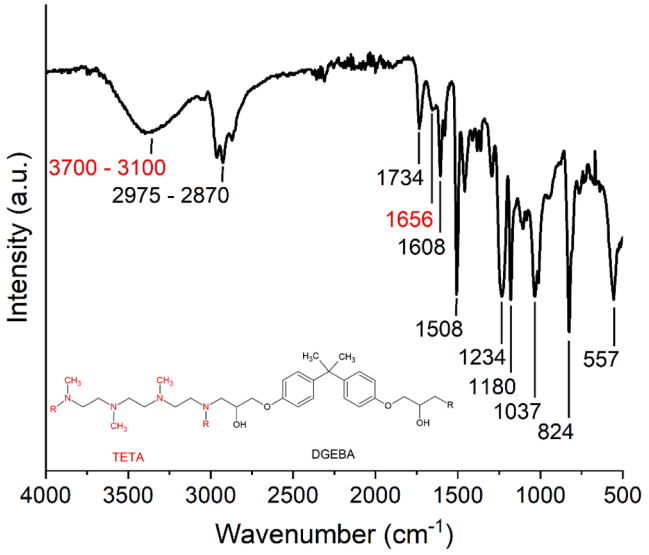

Fig. 2. FTIR spectra of DGEBA-TETA coating after curing highlighting the vibrations of primary and secondary amines. Inset: representative structure of DGEBA-TETA.

indicates the successful cure of DGEBA by TETA [32,33]. The appearance of a band at 1656 cm^{-1} and the vibrations in the range 3700 – 3100 cm^{-1} reveal the reaction with the hardener for the stretching of N—H groups of primary and secondary amines, respectively [30,33].

The effect of polishing, acid and alkaline etching, sol-gel primer, and anodizing on the roughness of aluminum alloys and steel was evaluated by atomic force microscopy (AFM) along with SEM. Higher surface roughness might play a role in mechanical adhesion by increasing the interfacial bond area, but it does not necessarily imply a superior anti-corrosion barrier [5,27]. Fig. 3 depicts the 3D AFM maps obtained over a 5 μm^2 area for the neat surfaces of the AA7075, AA2024 alloys and steel. The AA7075_reference and AA2024_reference samples presented similar roughness features with values around 38.4 nm and 37.5 nm, respectively, but a lower roughness was determined for steel_reference (16.9 nm) (Fig. 3a to c). The application of alkaline etching seems to favor the formation of an aluminum oxide layer (Fig. 3d to f), slightly decreasing the roughness of both aluminum alloys. The acid pre-treatment (Fig. 3g to i) promoted surface texturing and partial removal of the native oxide layer of AA7075, resulting in a higher R_{RMS} compared to the AA7075_reference. However, this effect was not so evident in AA2024 substrate, as observed in the comparative chart in Fig. 3o to p. A different regime is observed for steel, where both alkaline and acid etching increased the roughness by removing the iron oxide layer (Fig. 3f, i and q).

AFM maps of anodized aluminum surfaces could not be obtained due to heterogeneities and excessively rough profiles that could damage the AFM probe. However, SEM images confirm the formation of channels and large pores, with sizes varying between 100 nm and 1 μm (Fig. 3m and n). The increased contact area of anodized surfaces and pore size seem to be critical for coating adhesion. This has been previously explained by Abrahami et al. [27], who found that 20 nm was the minimum pore size for the epoxy resin to fill the pores and contribute to mechanical interlock. Finally, the application of a sol-gel layer/primer filled the cavities and pores of the neat aluminum and steel surfaces resulting in a sharp decrease in R_{RMS} values and a clear smoothing relative to the other samples (5.2 nm, 15.5 nm, and 6.5 nm for sol-gel_AA7075, sol-gel_AA2024 and sol-gel_steel, respectively).

The changes in roughness induced by the anodizing process were reflected in the hydrophilic character of treated aluminum alloys. Fig. 4a and b show a sharp decrease (nearly halved) in the water contact angle (WCA) values of the anodized surface compared to the other pre-treatments due to surface chemistry and/or increased roughness. The other pre-treatments on aluminum samples showed a slight increase in the WCA relative to the references, possibly due to changes in the acid-base properties at the surface. This can also depend on the chemical composition of the metal oxide [27]. For instance, an increase in hydrophobicity can correspond to the presence of functional groups or the density of hydroxyls groups, which act as coupling agents bonding metal/epoxy interfaces [27]. A similar trend is shown for WCA values on steel, except for the steel_alkaline specimen (Fig. 4c).

The morphology, homogeneity, and thickness of the DGEBA coatings were examined by SEM. Fig. 5 shows cross-sectional images obtained for coatings on AA7075, AA2024, and steel alloys and their respective average thicknesses in a bar chart in Fig. 5o to q. Regardless of the pre-treatment, all coatings were homogeneous and pore-free, which are essential characteristics for barrier coatings. The images reveal that the total thickness of AA7075 ranges approximately between 5 and 15 μm. An increase in thickness for AA7075 is observed in the sequence: reference < alkaline < acid < anodized < silane (Fig. 5o). A two-layer system was identified for the anodized sample, with an inner layer of about 8 μm thick and an epoxy topcoat of about 4.5 μm (Fig. 5m). On AA2024, the total thickness decreased in the order alkaline > sol-gel > anodized > acid > reference with values between 8 and 16 μm (Fig. 5p). Again, a thick layer was formed in the process of anodization with the inner layer (9.5 μm) covered by a 3.5 μm thick epoxy coating (Fig. 5n).

For the DGEBA coatings on steel, the cross-sectional images in Fig. 5c reveal homogeneous coatings with thickness between 5 and 24 μm (Fig. 5q). The thickness increased in a similar manner as in aluminum alloys, namely, reference < alkaline < acid < sol-gel. A significant increase in thickness was observed for the sol-gel pre-treated substrate suggesting that the silica clusters [34], obtained through hydrolysis and condensation of TEOS [34,35] contribute to the bonding of DGEVA chains to the iron oxide native layer. A similar variation has been reported when TEOS was incorporated into DGEBA-siloxane-silica coatings [36]. The authors observed an increased film thickness (from 1.6 to 6.7 μm) when optimized synthesis conditions were applied, pointing to the reactive nature of DGEBA and TEOS [36]. Considering that the same sol (DGEBA-based, described in Section 2.2) was deposited on surfaces treated in a different way, the variance in thickness implies that surface modification has a direct impact on the molecular interaction of the polymer chains with the substrate.

Electrochemical analysis of epoxy-coated aluminum and steel alloys

Corrosion barrier properties of the DGEBA-based coatings were evaluated by electrochemical impedance spectroscopy (EIS) assays on a weekly basis. The coatings were immersed for one month in a 3.5% NaCl solution to investigate how different pre-treatments affect adhesion and anti-corrosion performance. Fig. 6b to f shows Bode plots of DGEBA coatings on AA7075 differently pre-treated substrates and their respective neat (untreated) surfaces in green curves. After 1 day of immersion, the acid, anodized, alkaline, and sol-gel samples present excellent corrosion protection, showing a capacitive behavior along almost the entire frequency range (black symbols). The impedance modulus values at low frequency ($|Z|_{lf}$) were 6 orders of magnitude higher than the uncoated surfaces (green curves) e.g., 97 GΩ cm^2, 60 GΩ cm^2, 42 GΩ cm^2, and 28 GΩ cm^2 for AA7075_sol-gel, AA7075_acid, AA7075_alkaline, and AA7075_anodized samples, respectively. Only the AA7075_reference (polishing pre-treatment) resulted in lower corrosion protection on the first day of immersion, which was also reflected in its performance over time. The AA7075_acid failed after 7 days and remained stable at about 33 MΩ cm^2 after 30 days. All the other pre-treatments (anodized, alkaline and sol-gel) resulted in high protection against corrosion for up to one month corroborated by the absence of a significant phase angle decay in Fig. 6d to f.

The first and last day curves obtained by EIS for DGEBA coatings on AA7075, AA2024 and steel were fitted using three different electrical

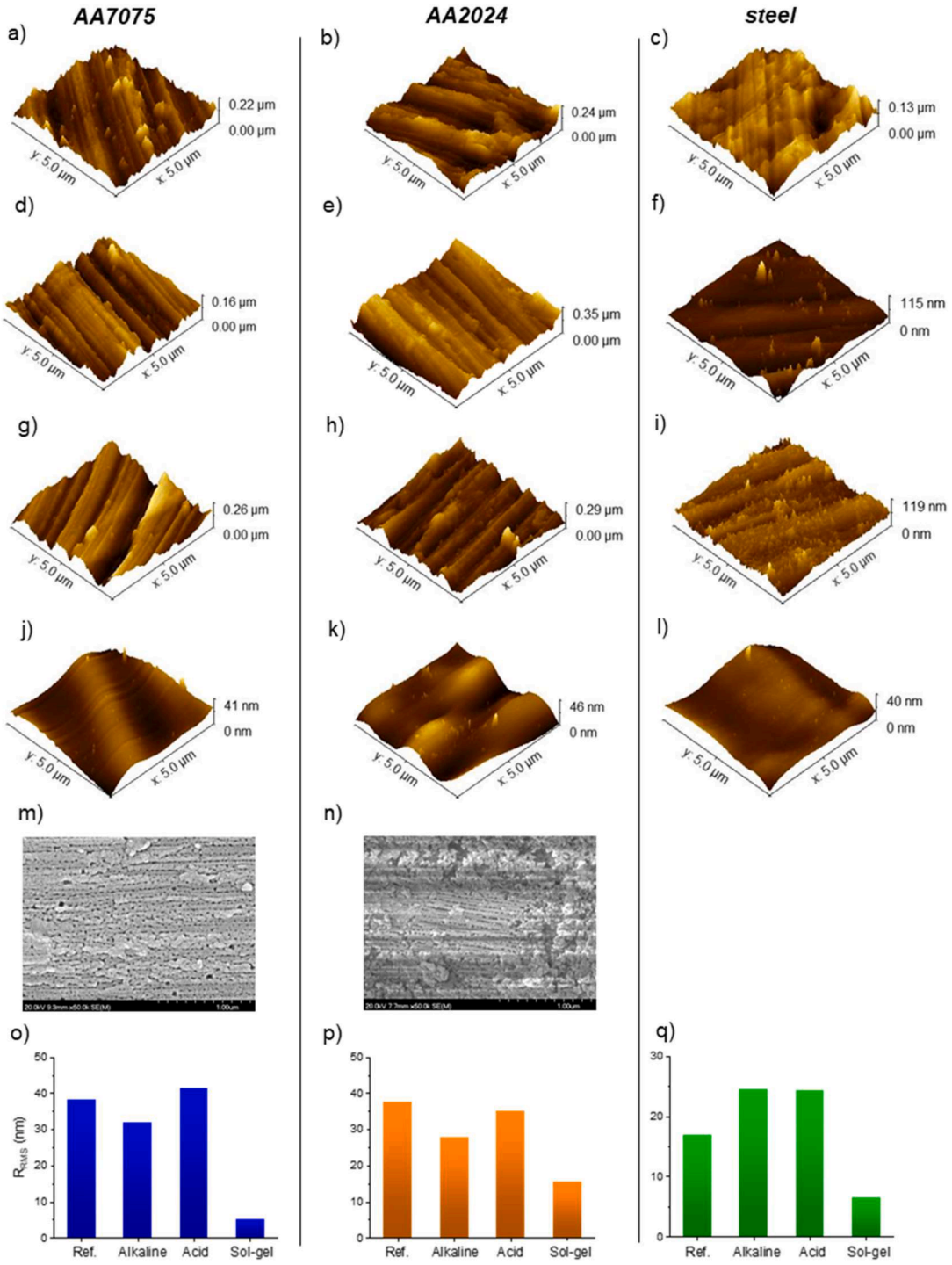

Fig. 3. 3D topographic images of AA7075, AA2024 and steel specimens respectively for a – c) reference, d – f) alkaline, g – i) acid, j – l) sol-gel, and m – n) anodizing pre-treatments by AFM and SEM. A comparative column chart of the roughness values by AFM (R_{RMS}) is depicted at the bottom (o – p).

equivalent circuits (EECs), depicted in Fig. 6a. The results are reported in Table S1. The EEC composed of one time constant was used to fit highly capacitive coatings, where almost no signs of degradation were observed. The symbol Rs is the solution resistance and R_1/CPE_1 represent the resistance and the capacitance of a barrier coating. The expansion of the resistive behavior at low frequencies was detected by extracting the breakpoint frequency (f_b) from the phase angle plots (black line at -45°, values in Table S1), defining the boundaries between capacitive and resistive regions [37,38]. At this stage, a second time constant (R_2/CPE_2) is added to the EEC to simulate the resistance and capacitance of an outer layer with pores and channels. Only when the coating failed due to pitting corrosion, a third time constant was used to represent the redox reactions at the coating/metal interface, described by charge transfer resistance (R_3) and the capacitance of the electrical double layer (CPE_3) [37,38]. As expected, the extracted values confirm the high performance of AA7075_alkaline, AA7075_anodized and AA7075_sol-gel coatings, with corrosion resistance ranging from 46.7 GΩ cm^2 to 478.3 GΩ cm^2 after one day of immersion.

Similar behavior was observed when DGEBA-based coatings were applied to pre-treated AA2024 alloys. Low-frequency impedance values

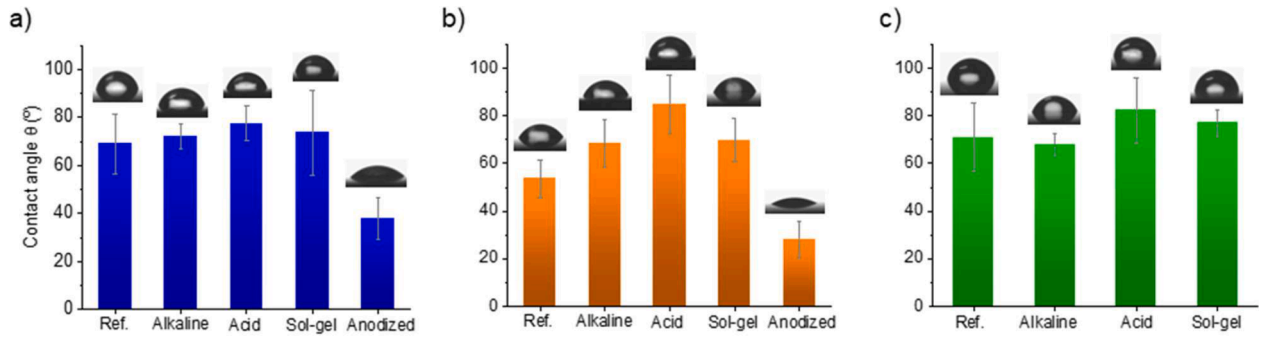

Fig. 4. Average water contact angle (WCA) of neat a) AA7075, b) AA2024 and c) steel substrates after different pre-treatments.

($|Z|_{lf}$) were as high as 107.1 GΩ cm^2, 71.8 GΩ cm^2, 71.7 GΩ cm^2, 32.2 GΩ cm^2 for the AA2024_sol-gel, AA2024_acid, AA2024_alkaline and AA2024_anodized, respectively, on the first day of immersion (Fig. 7b to e), which represents a 10^6 to 10^7-fold increase in comparison to the treated substrates without epoxy coating (green curves). Fig. 7 evidences an even greater discrepancy between the performance of these samples in relation to the AA2024_reference (Fig. 7a), whose $|Z|_{lf}$ after one day of immersion is 3 MΩ cm^2. Among these samples, only the AA2024_acid presents signs of light deterioration and water uptake after 29 days of immersion but still provides better protection than the AA2024_reference (polished treatment).

Fig. 8 shows the Bode plots for the epoxy coatings deposited on mild steel recorded over four weeks. Steel_alkaline, steel_acid and steel_reference (Fig. 8a to c) presented $|Z|_{lf}$ values of 17.6 GΩ cm^2, 2.2 GΩ cm^2, and 8.2 GΩ cm^2, respectively, on the first day of immersion. Even though the reference presented higher impedance in the initial period of immersion, the pristine barrier quickly deteriorated (3.8 MΩ cm^2 after 7 days, remaining stable until 29 days). This can be attributed to a faster water uptake process through the polymer chains, and poorer adhesion. On the other hand, the steel_sol-gel, Fig. 8d, showed a capacitive behavior over almost the entire frequency range during the studied period, reaching $|Z|_{lf}$ values as high as 126 GΩ cm^2, 7 orders of magnitude higher than that of the sol-gel treated steel without epoxy coating. A remarkable protective barrier is observed for this sample, as almost no degradation was observed during the immersion time.

Overall, the EIS analysis of the coating revealed an important influence of the pre-treatments on both aluminum and steel alloys: (i) pre-treatment plays an important role in the barrier properties since different performances were found for different surface finishing, (ii) sol-gel, alkaline and anodized treatments presented the best performance with a capacitive behavior over almost the entire frequency range during one month (on steel, however, only the sol-gel sample did not present deterioration), and (iii) the application of a sol-gel layer as surface treatment represents an excellent alternative for anti-corrosion applications considering its low complexity, energy expenses, ease of storage and preparation.

Mechanical analysis and pull-off adhesion of epoxy-coated aluminum and steel alloys

Micro-scratch measurements were carried out to assess the mechanical properties of the epoxy coatings on aluminum alloys and steel, including the determination of the coefficient of friction and the coating adhesion, which scales with the critical load of delamination (Lc). The scratch tests were performed with increasing load (1–10 N) over a 3 mm track, and the results are summarized in Figs. 9 to 11. The micro-scratch plots of AA7075 and their corresponding images reveal that AA7075_anodized, AA7075_reference, and AA7075_acid presented failure events with Lc values of 4.3, 4.7, and 6.8 N, respectively. The coatings on AA7075_alkaline and AA7075_sol-gel did not present any crack or delamination along the scratch, indicating their excellent adhesion to the substrate (Fig. 9a). This result is possibly related to a higher fraction of hydroxyl groups from the alkaline etching that promotes hydrogen bonds and to the presence of silica clusters from sol-gel thus covalently bonding the polymer and metal oxide [11,13,36]. The coefficient of friction (Fig. 9b) presented similar values for all measured samples, varying between 0.1 and 0.2 over the entire scratch track.

The same procedure was applied to the coated AA2024 specimens, and the results depicted in Fig. 10 show a failure only for the AA2024_reference. The decrease in the Lc value of the AA2024_reference compared to AA7075_reference (3.4 N lower) indicates poorer adhesion. This result is in line with the lower anti-corrosion performance detected by EIS on the first day of immersion (Fig. 7a). Notably, even though AA2024_acid is thicker than AA7075_acid (8.0 μm vs. 5.2 μm, respectively), the film thickness seems not to play the primary role in adhesion. The alloy composition also reflected in differences in the WCA, might contribute to adhesion and consequently to the barrier property. For the AA2024_anodized, there seems to be higher tension at the end of the scratch, but no failure was detected for the applied load. These coatings are also characterized as low friction coatings with coefficient values below 0.2 (Fig. 10b).

The micro scratch analysis of epoxy coatings on steel in Fig. 11 shows a failure only of the steel_reference, with a Lc of 6.7 N. This relatively high Lc value of steel compared to those observed for aluminum alloys agrees with the electrochemical response. After one day of immersion, the steel_reference presented a $|Z|_{lf}$ of 8.2 GΩ cm^2 compared to 0.6 GΩ cm^2 and 0.003 GΩ cm^2 of AA7075_reference and AA2024_reference, respectively, confirming the strong dependence between the barrier properties, adhesion and nature of the substrate. The coatings on steel_acid, steel_alkaline and steel_sol-gel did not present any cracks or delamination along the scratch due to their improved adhesion to the substrate. The coefficient of friction was similar for all samples, with values between 0.1 and 0.2 over the entire track (Fig. 11b).

The tensile pull-off force of epoxy films on the three studied substrates was evaluated following ASTM D4541–17. An Elcometer 510 pull-off adhesion tester measured the detachment force of aluminum dollies glued to dry (as prepared) and wet coatings (after 30 days of immersion in 3.5% NaCl). The results are summarized in Table 2 and the images illustrating adhesive, cohesive and glue failures are shown as Figure S2. All results demonstrate a weaker adhesion of coatings after immersion in saline solution test due to water-polymer interaction causing chain relaxation [39]. An adhesive failure occurred on wet AA7075_reference, steel_reference and AA7075_anodized, leaving the coatings on the dolly and a bare substrate. Thus, it was not possible to measure the pull-off adhesion for these samples. The sharpest decrease in adhesion before and after immersion is observed for DGEBA coatings on steel_acid and AA2024_reference, with a 3 to 4-fold decrease of measured values. The adhesion strength of all the other coatings was approximately halved after immersion, while the epoxy films on AA7075 showed the best results: the decrease in adhesion was only 1.2 to 1.4 times.

Alkali, acid, anodization and sol-gel pre-treatments resulted in the

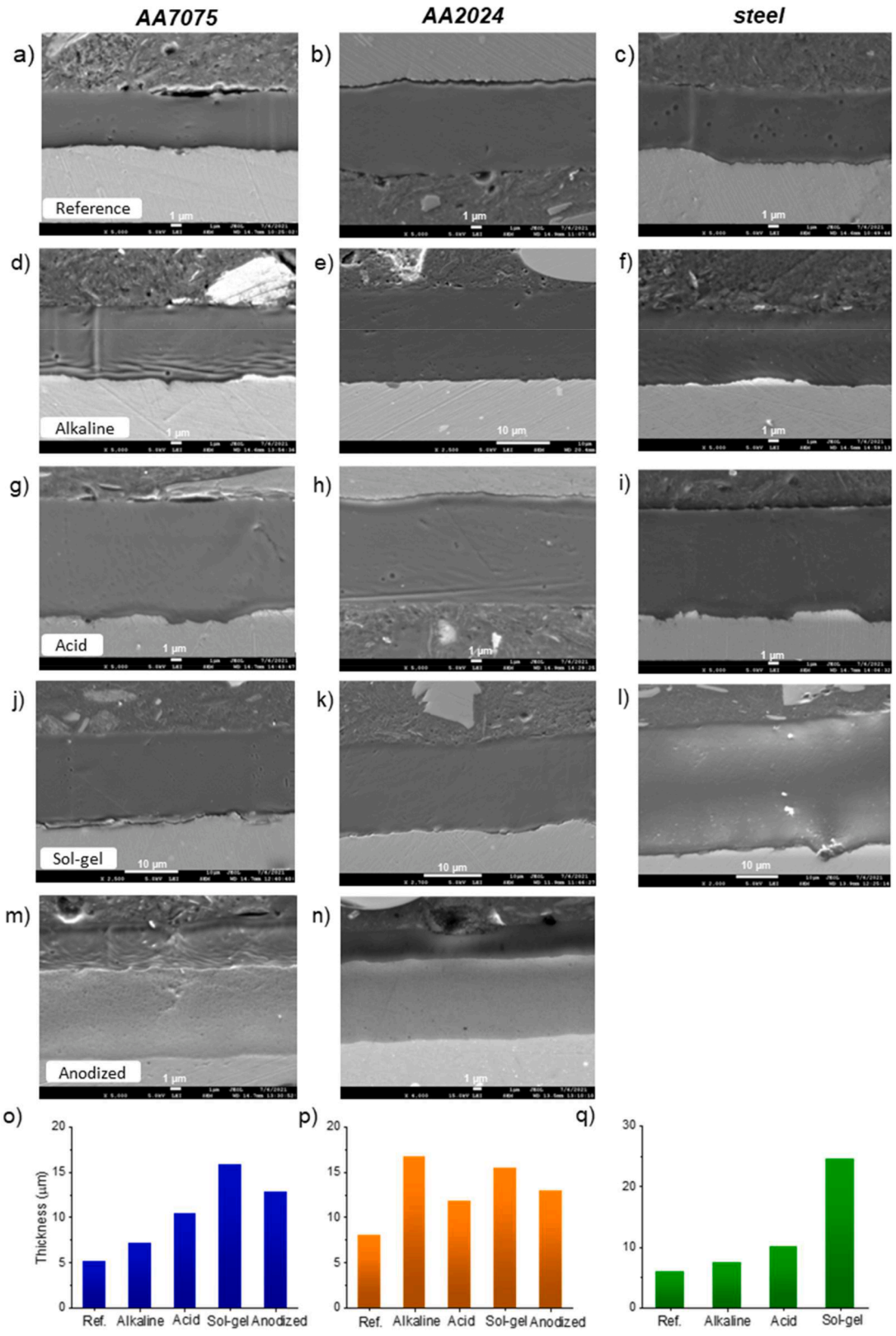

Fig. 5. Cross-sectional SEM images of DGEBA coatings on a) AA7075, b) AA2024 and c) steel after different pre-treatments and average thicknesses in comparative charts.

best dry adhesion of coatings on aluminum alloys, with values of up to 14.5 MPa (AA2024_alkaline). These results correlate with the anti-corrosion performance reported above. A slight discrepancy between EIS and pull-off adhesion is detected for the dry steel_reference, whose adhesion values are comparable to those of dry coatings on aluminum (5.4 MPa). However, more severe water uptake and consequent polymer detachment took place in the epoxy-steel interface, resulting in complete detachment (Figure S2).

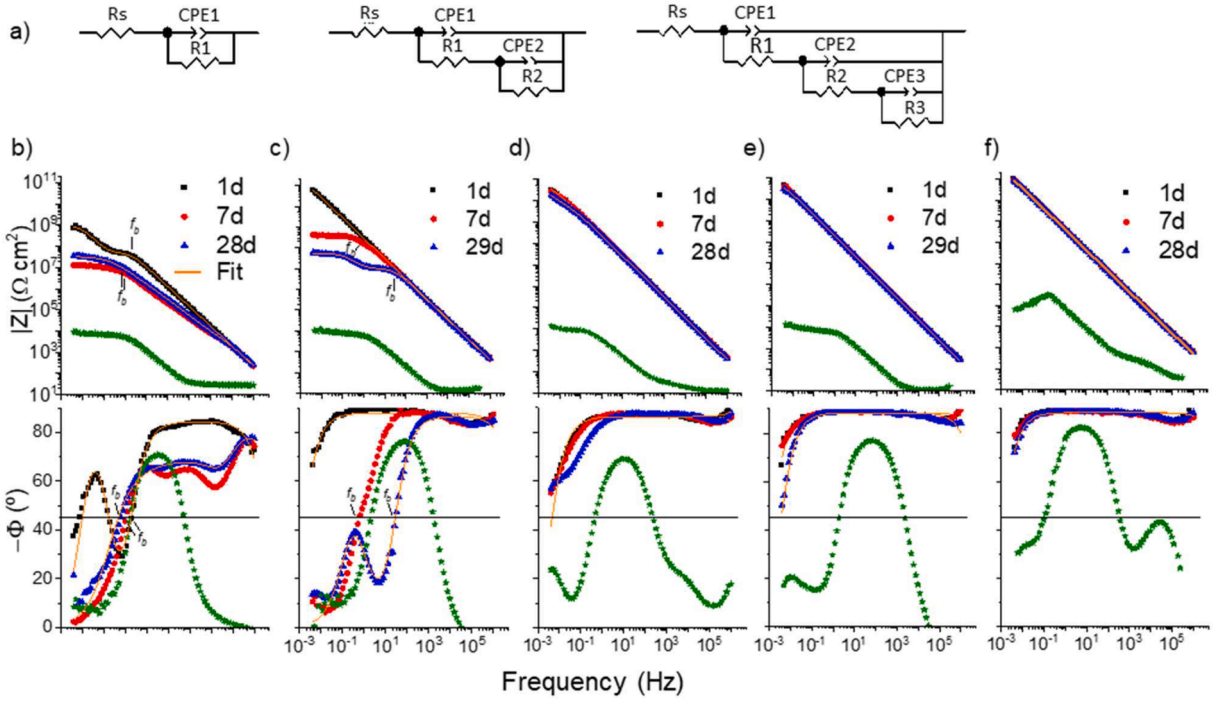

Fig. 6. a) Electrical equivalent circuits used to fit (orange lines) the EIS data of DGEBA coatings on a) reference, b) acid, c) anodized, d) alkaline, and e) sol-gel treated surfaces on AA7075 as a function of immersion time in 3.5 wt.% NaCl. The EIS of pre-treated surfaces without epoxy coating is shown in green.

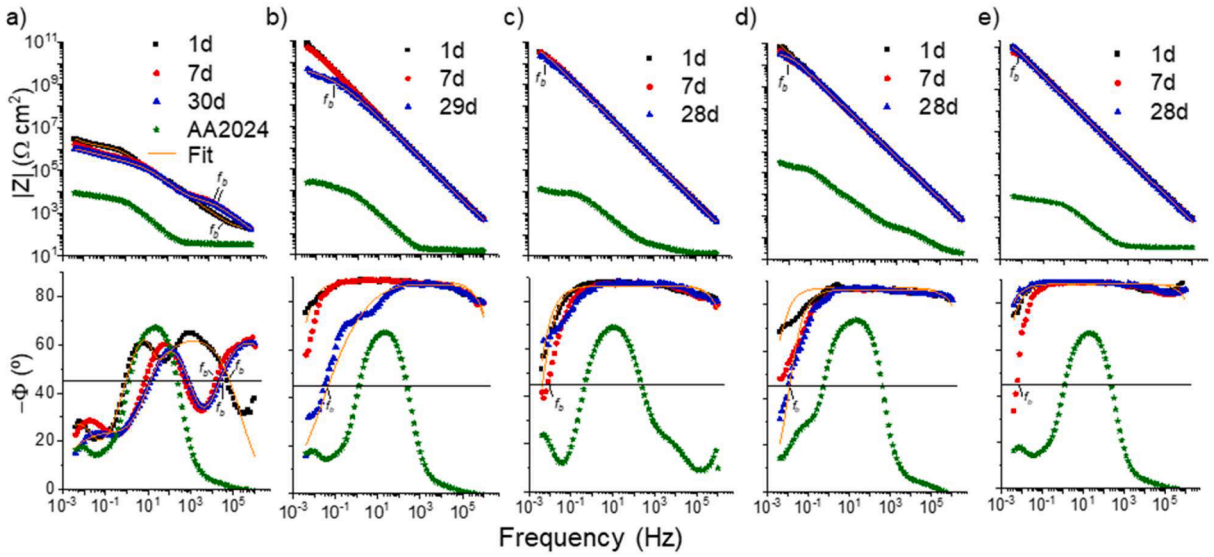

Fig. 7. Bode plots of DGEBA coatings on a) reference, b) acid, c) anodized, d) alkaline, and e) sol-gel treated surfaces on AA2024 as a function of immersion time in 3.5 wt.% NaCl. The EIS of pre-treated surfaces without epoxy coating is shown in green.

The Pull-off results in Table 2 indicate a clear enhancement of dry adhesion for all pre-treated surfaces compared to the polished reference especially on aluminum surfaces e.g., 75% improvement on AA7075_acid, and 61% on AA2024_alkaline. For steel, however, only about a 14% increase in dry adhesion is detected relative to the reference (steel_sol-gel). Recent studies of conversion coatings containing cerium-neodymium (Ce-Nd) incorporated into a polyester/melamine coating have shown promising results on steel [40]. The authors found a 57% improvement in dry adhesion compared to the untreated surface accompanied by a slightly higher anti-corrosion performance (one order of magnitude increase of $|Z|_{lf}$) [40]. Interesting outcomes for epoxy coatings on steel were found for a conversion coating based on europium oxide (Eu_2O_3) [41]. No cohesive failure is observed for the conversion coated steel along with about 58% improvement of the resistance against cathodic disbondment. An increase of $|Z|_{lf}$ from approximately 5 GΩ cm^2 to about 50 GΩ cm^2 after one day of immersion in 3.5% NaCl solution suggests the potential of these eco-friendly conversion coatings [41].

By gathering surface, mechanical and electrochemical results (Table 3), we can draw a comparative analysis and propose a bonding mechanism for each system. Recapping the previous discussion, differences between the roughness of neat substrates are observed. The applications of a sol-gel primer filled up the pores and heterogeneities of both steel and aluminum alloys, thus reducing their surface roughness.

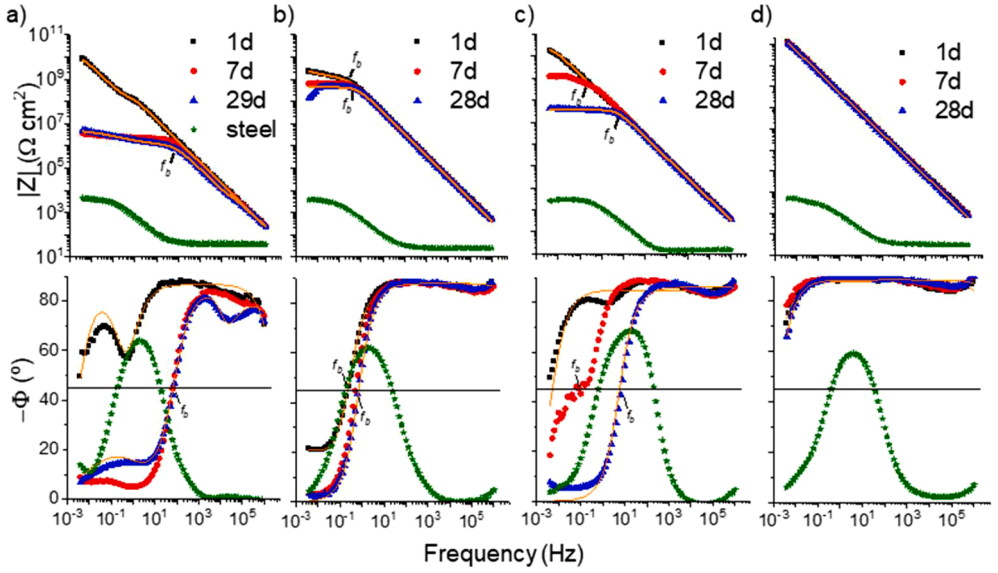

Fig. 8. Bode plots of DGEBA coatings on different steel treated surfaces as a function of immersion time in 3.5 wt.% NaCl. The coatings immersed for one month are depicted as a) reference, b) acid, c) alkaline, and d) sol-gel. The EIS of pre-treated surfaces without epoxy coating are shown in green.

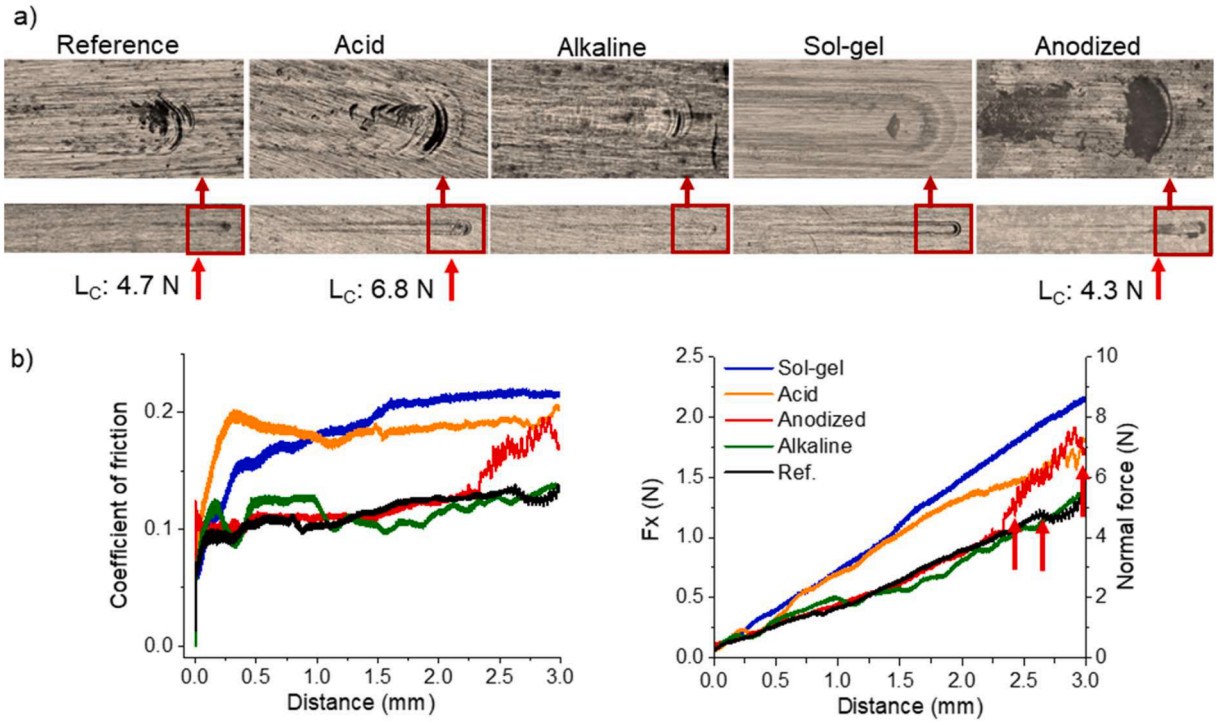

Fig. 9. a) Scratch tracks of DGEBA coatings on AA7075 by optical microscopy and b) coefficient of friction and critical load of delamination plots.

Furthermore, WCA values are significantly lower for anodized samples due to their high roughness and the presence of channels/pores that interact with water. The application of a sol-gel primer and mild alkaline etching on aluminum alloys provided functional groups that increased the hydrophobicity compared to the WCA of reference samples. On the other hand, the depletion of hydroxyl groups driven by the acid etching [26] might have contributed to interactions between the surface and water, resulting in higher WCA values for all substrates. The WCA values of steel were similar for all neat surfaces, ranging between 68° (alkaline) and 82° (acid).

Mechanical failures were observed only for epoxy coatings on AA7075_acid, AA7075_anodized, and all the references (Table 3). The loss of adhesion after 30 days of immersion is documented by the ratio between the dry and wet adhesion obtained by pull-off tests. The results point to sol-gel and alkaline etching as the most efficient surface treatments for all specimens. Acid etching on AA7075 and AA2024 alloys also performed fairly well. However, this is not reflected in the barrier properties, as explained below.

The thickness measurements (Fig. 5) and the results of electrochemical analysis (Figs. 6 to 8) point out that thicker coatings result in improved barrier properties. Nevertheless, the observed coating performance is not solely explained by a thickness effect but also by other

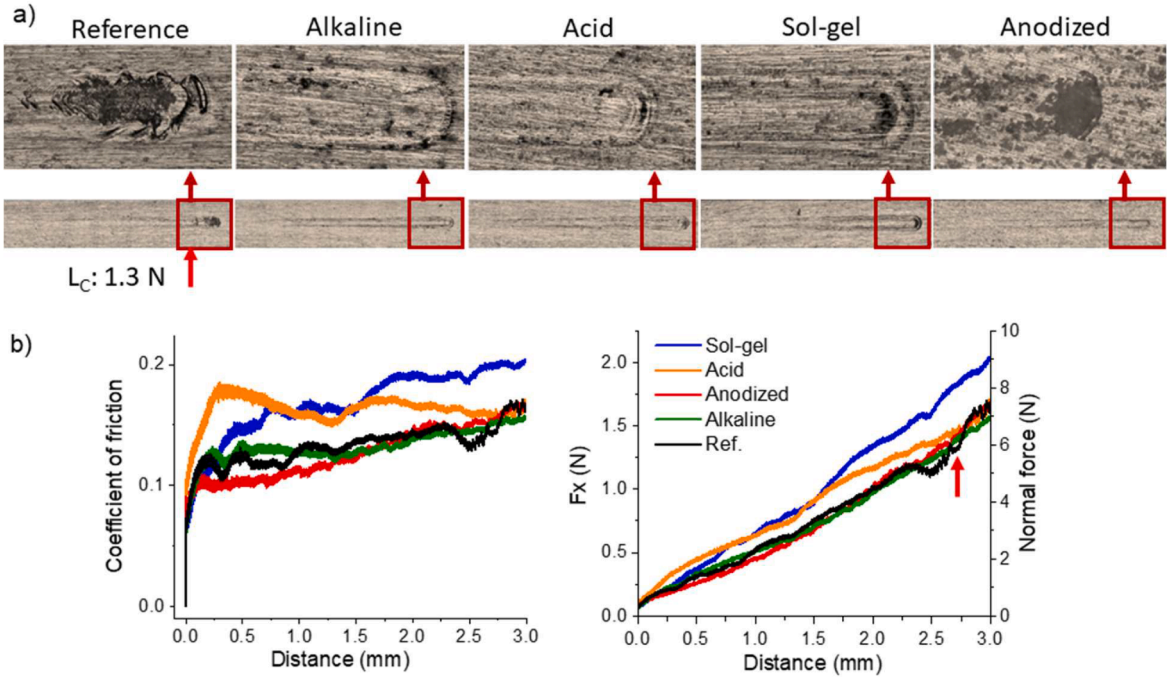

Fig. 10. a) scratch tracks of DGEBA coatings on AA2024 by optical microscopy and corresponding b) coefficient of friction and critical load of delamination plots.

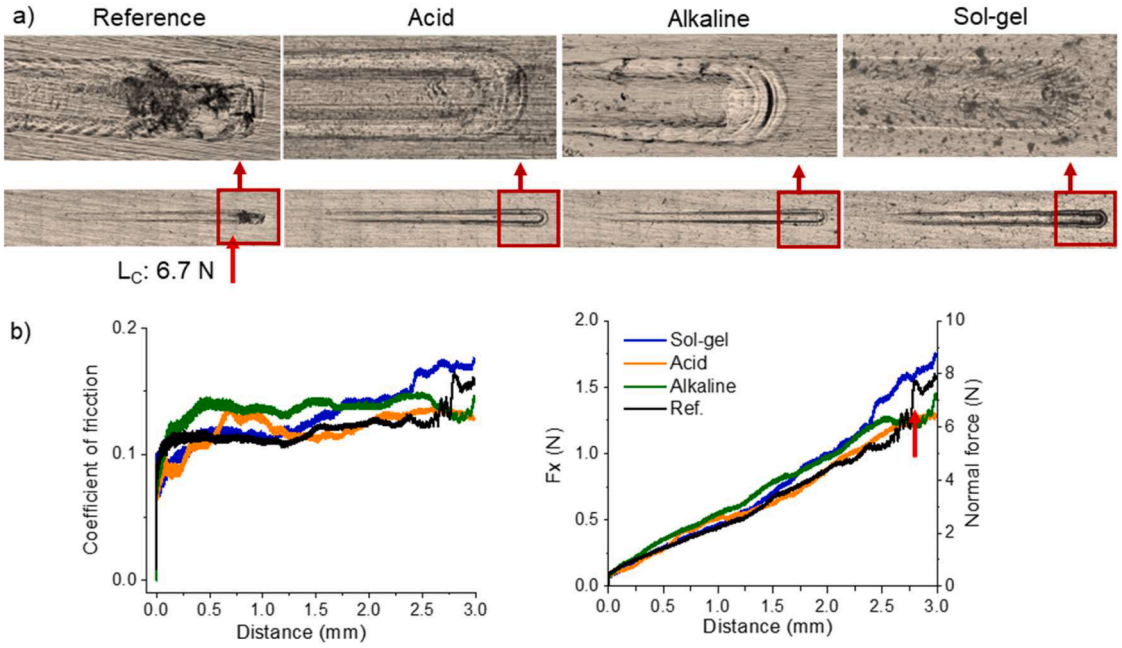

Fig. 11. a) Scratch tracks of DGEBA coatings on mild steel by optical microscopy and corresponding b) coefficient of friction and critical load of delamination plots.

factors, such as coating porosity, polymer crosslinking, and adhesion to the substrate. Therefore, to make a fair comparative analysis, we weighted the corrosion performance (low-frequency impedance values) by the thickness ($|Z|_{lf}$ _1d/d, Table 3). These ratios show an excellent correlation for the treatments on aluminuim, namely, the sol-gel primer, alkaline and acid etching, which resulted in the best barrier properties, with $|Z|_{lf}$ above 4 GΩ cm^2. Only the epoxy coating on steel_sol-gel presented a similar performance (5 GΩ cm^2).

Finally, we studied the time dependence of the barrier properties by determining the $|Z|_{lf\_1d}/|Z|_{lf\_28d}$ ratios after dividing the impedance values obtained on the first day by the values from the 28th day of immersion. The smaller this ratio is, the slower the coating degrades. Almost no water uptake was observed by EIS for AA7075_sol-gel (1.1), AA7075_alkaline (1.3), and AA7075_anodized (1.6-fold decrease), which is in line with the results observed for epoxy coatings on AA2024 (1.0, 2.1 and 1.4-fold decrease, respectively). On steel, however, only the epoxy coating on the sol-gel pre-treatment presented a low water uptake (1.1-fold decrease), which is significantly smaller than the values observed for the other pre-treatments.

The presence of channels and pores with sizes varying between 100 nm and 1 μm in the anodized samples resulted in a higher roughness and low WCA of these surfaces. Mechanical and adhesion failures observed

Table 2
Pull-off adhesion values of epoxy-coated AA7075, AA2024 and carbon steel before and after immersion in 3.5% NaCl solution. Blank cells correspond to failed coatings. The values are in MPa.

	AA7075 (MPa)		AA2024 (MPa)		Steel (MPa)	
	Dry	Wet	Dry	Wet	Dry	Wet
Reference	2.98	–	5.58	1.30	5.40	–
Alkaline	10.68	8.23	14.50	6.99	3.14	1.87
Acid	12.37	10.42	8.58	5.80	4.40	1.42
Sol-gel	9.59	6.87	5.82	3.38	6.32	2.72
Anodized	8.97	–	9.04	4.21	N/A	N/A

N/A: not applicable.

Table 3
Film roughness, water contact angle (WCA), thicknesses, critical load of delamination (Lc), dry/wet adhesion ratio, low-frequency impedance modulus ($|Z|_{lf}$) after 1 day of immersion, ($|Z|_{lf\_1d}$) normalized by the thickness, and ($|Z|_{lf}$) ratio ($|Z|_{lf\_1d}$ / $|Z|_{lf\_28d}$). Values obtained by AFM, water contact angle measurements, SEM, micro-scratch test and EIS.

		Sol-gel	Alkaline	Acid	Anodized	Reference
AA7075	Roughness (nm)	5.2	32.0	41.3	–	38.4
	WCA (°)	73	72	77	38	69
	Thickness (μm)	15.7	7.2	10.5	12.9	5.2
	L_C (N)	–	–	6.8	4.3	4.7
	Adhesion loss $_{dry/wet}$	1.4	1.3	1.2	–	–
	$\|Z\|_{lf\_1d}$ (GΩ cm^2)	97.2	42.0	60.1	28.8	0.6
	$\|Z\|_{lf\_1d}$/ d (GΩ cm^2)	6.1	5.8	5.7	2.2	0.1
	$\|Z\|_{lf\_1d}$ / $\|Z\|_{lf\_28d}$	1.1	1.3	1000	1.6	20
AA2024	Roughness (nm)	15.5	27.9	35.0	–	37.3
	WCA (°)	70	68	85	28	53
	Thickness (μm)	15.5	16.5	12.0	13.0	8.0
	L_C (N)	–	–	–	–	1.3
	Adhesion loss $_{dry/wet}$	1.7	2.0	1.5	2.1	4.3
	$\|Z\|_{lf}$ (GΩ cm^2)_1d	107.1	71.7	71.8	33.1	0.003
	$\|Z\|_{lf\_1d}$/ d (GΩ cm^2)	6.9	4.3	5.9	2.5	3.7×10^{-4}
	$\|Z\|_{lf\_1d}$ / $\|Z\|_{lf\_28d}$	1.0	2.1	14.8	1.4	3.0
Steel	Roughness (nm)	6.5	24.5	24.3	*	16.9
	WCA (°)	77	68	82	*	71
	Thickness (μm)	25.1	7.4	10.2	*	6.0
	L_C (N)	–	–	–	*	1.3
	Adhesion loss $_{dry/wet}$	2.3	1.6	3.0	*	–
	$\|Z\|_{lf}$ (GΩ cm^2)_1d	126.2	17.6	2.2	*	8.2
	$\|Z\|_{lf\_1d}$/ d (GΩ cm^2)	5.0	2.3	0.2	*	0.5
	$\|Z\|_{lf\_1d}$ / $\|Z\|_{lf\_28d}$	1.1	440	15.7	*	810

* not applicable.

for the epoxy coating on AA7075_anodized suggest that the predominant adhesion mechanism, in this case, is mechanical interlocking [4,5,8,11]. Previous works investigated the effect of surface roughness, contact area, oxide thickness, pore size and hydrophobicity and concluded that predominant factors for good adhesion rely on the formation of a fully cohesive interphase [27]. In other words, complete pore filling reduces the presence of nano- and microvoids, decreasing the susceptibility of water-polymer interactions at the polymer-metal interface [39]. Nonetheless, the anodizing procedure performed in this work resulted in materials with a good barrier with low water uptake, as can be observed from the EIS tests and the results in Table 3.

Acid–base interactions, e.g., hydrogen bonds, are considered to play a major role within the adsorption theory. Hydrogen bonds can form between an interfacial donor and the acceptor of an electron pair [4]. The structure of DGEBA has available hydroxyl groups which are thought to form hydrogen bonds on the aluminum oxide surface. Additionally, the presence of basic nitrogen electron pairs from hardeners, such as tetraethyl amine (TETA) used in this work as hardener, can contribute to adhesion via Lewis or Bronsted interactions [42]. Typically, two different bonding modes between the amine nitrogens and the oxide surface are observed: via Lewis interactions between basic N lone pair electrons and acidic metal (acid etching) and Bronsted interactions between hydroxyls (e.g. available groups from DGEBA and the metal surface – alkaline etching) and nitrogenous lone-pair electrons (nitrogen protonation) contributing further to improving the adhesion [5,42]. Therefore, the amount of hydroxyl groups available at the oxide surface has a direct impact on the adsorption mechanism and bonding of epoxy resins [5].

Table 1 suggests that physical interactions (Van der Waals forces) and hydrogen bonds are the main driving forces for epoxy adhesion on reference (polished), alkaline and acid-treated surfaces. AFM and WCA analysis did not reveal any big discrepancies in these systems, but a marked difference in the thickness of the epoxy coatings suggests changes in molecular interactions with the polymer chains due to the presence of specific functional groups or different hydroxyl densities [4, 27]. The higher hydroxyl density provided by alkaline etching could explain the good adhesion and barrier properties of epoxy coatings on aluminum, thus confirming the hydrogen bonds hypothesis. Regarding the acid etching, it has been reported that acid cleaning (1 mM HNO_3) of ZnMgAl alloy lowered the hydroxide concentration and increased the metal ion concentration, fostering Lewis interactions [26]. Therefore, the improvement of DGEBA coatings on acid (HCl, pH 2) and alkaline (KOH, pH 11.5) etching was directly proportional to the number of hydrogen bonds that led to proper polymer anchoring but through different mechanisms: Lewis interactions for acid etching, and Bronsted interactions for alkaline etching.

The acidic hydrolysis and condensation of silica clusters (sol-gel treatment) resulted in a significant improvement in the adhesion and barrier properties of DGEBA coatings regardless of the substrate. This performance can be attributed to metal-silane bonds of the type Me-O-Si [13] but also to a possible side reaction between the primer and the epoxy coating forming a “hybrid” structure during the thermal treatment of the coatings (60 and 160 °C, session 2.2). Covalent epoxy-metal oxide bonds have granted excellent anti-corrosion protection to both aluminum and steel alloys. The low-frequency impedance modulus reach values of about 6 orders of magnitude higher than uncoated substrates. This confirms that the presence of functional groups prevailed over such factors as surface roughness, contact area, oxide layer thickness, pore size and hydrophobicity.

Regarding the coatings on steel, all samples presented a good barrier against corrosion on the first day of immersionbut only the sol-gel treatment showed almost no signs of degradation over time. High $|Z|_{lf\_1d}$ / $|Z|_{lf\_28d}$ ratio was detected for steel_alkaline and steel_acid (440 and 15.7, respectively) pointing to the rapid degenerative nature of DGEBA coatings on these surface finishes, whose bonding mechanism is associated with hydrogen bonds. As no mechanical failures were observed in these coatings during the microscratch test, we can postulate that although hydrogen bonds promote good adhesion to steel, these connections are not strong or stable enough to form an impermeable barrier such as those on aluminum alloys (especially for the alkaline pretreatment). This means that covalent bonds are essential to ensure good barrier and mechanical properties of epoxy coatings on both steel and aluminum alloys.

Conclusions

A systematic analysis of DGEBA-based coatings on mild steel and aluminum alloys modified by five independent methods revealed that the pre-treatment stage has a direct impact on the molecular interactions between the polymer and metal oxide. The surface modifications, similar to those employed in commercial applications, resulted in distinct adhesion and barrier performances, making it possible to correlate them with coatings' properties and bonding mechanisms.

1 Mechanical etching (polishing) bonds the epoxy film to iron and aluminum oxides mostly through physical interactions, and mechanical interlocking. The obtained roughness and texture surface, however, are not able to guarantee adhesive anchoring of the epoxy chains resulting in poor corrosion protection and adhesive failure on AA7075 and mild steel.
2 Chemical etching using an acid solution enhances the surface reactivity by depleting hydroxyls density. Good dry adhesion, especially on AA7075 (12.3 MPa), and fair anti-corrosion performance is observed in the short term, but coating degradation occurs on all substrates. In contrast, alkaline etching not only improves the anti-corrosion performance of DGEBA coatings but also promotes strong adhesion, particularly to dry AA2024 (14.5 MPa) and AA7075 (10.6 MPa). This is due to increased hydroxyl density that fosters hydrogen bonds via Bronsted interactions. Despite hampering the ingress of water, a slightly lower anti-corrosion performance is observed on steel.
3 Channels and porosity sizing from 100 nm to 1 μm are obtained by anodizing aluminum alloys in an oxalic acid solution. The additional structure imparts beneficial effects on the barrier properties of epoxy coatings on both alloys, but coating delamination is observed on AA7075 by applying a 4.3 N load along with adhesive failure after one month of immersion. Mechanical interlocking, known as the major boding mechanism in anodized layers, seems to lead to a tangible barrier and good adhesion but limited mechanical strength.
4 The application of sol-gel primer led to an insignificant water uptake of DGEBA coatings for all substrates during 30 days of immersion, which is in line with the excellent mechanical strength and adhesion of the coatings. Covalent bonds, provided by organosilanes, have proved superior performance without adverse environmental impact. As a result, such surface modification can conciliate high-performance coatings and environmental care.

Declaration of Competing Interest

The authors declare the following financial interests/personal relationships which may be considered as potential competing interests:

Dusan Galusek reports financial support was provided by EU Framework Programme for Research and Innovation Spreading Excellence and Widening Participation. Amir Pakseresht reports financial support was provided by Slovak Academy of Sciences.

Data availability

Data will be made available on request.

Acknowledgements

The authors acknowledge the financial support from the European Unionś Horizon 2020 Research and Innovation Programme under grant agreement No 739566, project FunGlass. Additionally, the funding obtained from VEGA 1/0171/21 and VEGA 1/0241/23 is acknowledged. This article is also part of the dissemination activities of MICINN project TED2021-131258B-I00. The colleagues assisting in the experiments: Mgr. Peter Švančárek, Ing. Dagmar Galusková, Mr. David Soriano Barrio, Dr. Sara Serena Palomares, Nilo Cornejo and Emilia Merino are kindly thanked.

Supplementary materials

Supplementary material associated with this article can be found, in the online version, at doi:10.1016/j.apsadv.2023.100479.

References

[1] S. Kumar, S. Krishnan, S.K. Samal, S. Mohanty, S.K. Nayak, Toughening of petroleum based (DGEBA) epoxy resins with various renewable resources based flexible chains for high performance applications: a review, Ind. Eng. Chem. Res. 57 (2018) 2711–2726, https://doi.org/10.1021/acs.iecr.7b04495.
[2] E. Savonnet, E. Grau, S. Grelier, B. Defoort, H. Cramail, Divanillin-based epoxy precursors as DGEBA substitutes for biobased epoxy thermosets, ACS Sustain. Chem. Eng. 6 (2018) 11008–11017, https://doi.org/10.1021/acssuschemeng.8b02419.
[3] A.A. Almusallam, F.M. Khan, S.U. Dulaijan, O.S.B. Al-Amoudi, Effectiveness of surface coatings in improving concrete durability, Cem. Concr. Compos. 25 (2003) 473–481, https://doi.org/10.1016/S0958-9465(02)00087-2.
[4] M.P. Martínez-Viademonte, S.T. Abrahami, T. Hack, M. Burchardt, H. Terryn, A review on anodizing of aerospace aluminum alloys for corrosion protection, Coatings 10 (2020) 1–30, https://doi.org/10.3390/coatings10111106.
[5] J.P.B. van Dam, S.T. Abrahami, A. Yilmaz, Y. Gonzalez-Garcia, H. Terryn, J.M. C. Mol, Effect of surface roughness and chemistry on the adhesion and durability of a steel-epoxy adhesive interface, Int. J. Adhes. Adhes. 96 (2020), https://doi.org/10.1016/j.ijadhadh.2019.102450.
[6] M. Droździel-Jurkiewicz, J. Bieniaś, Evaluation of surface treatment for enhancing adhesion at the metal–composite interface in fibre metal-laminates, Materials 15 (2022), https://doi.org/10.3390/ma15176118.
[7] A. Farooq, A. Hannan, R. Ahmad, K.M. Deen, The effect of chemical treatment on the adhesion strength and structural integrity of the epoxy coatings, Surf. Topogr. 9 (2021), https://doi.org/10.1088/2051-672X/ac443c.
[8] H. Wei, J. Xia, W. Zhou, L. Zhou, G. Hussain, Q. Li, K. Ostrikov, Adhesion and cohesion of epoxy-based industrial composite coatings, Compos. B Eng. 193 (2020), https://doi.org/10.1016/j.compositesb.2020.108035.
[9] M. Hamdi, M.N. Saleh, J.A. Poulis, Improving the adhesion strength of polymers: effect of surface treatments, J. Adhes. Sci. Technol. 34 (2020) 1853–1870, https://doi.org/10.1080/01694243.2020.1732750.
[10] W. Chandler, Pros and cons of alkaline vs. Acid etching of aluminum, Met. Finish. 106 (2008) 15–18, https://doi.org/10.1016/S0026-0576(08)00031-7.
[11] S.T. Abrahami, T. Hauffman, J.M.M. De Kok, J.M.C. Mol, H. Terryn, Effect of anodic aluminum oxide chemistry on adhesive bonding of epoxy, J. Phys. Chem. C 120 (2016) 19670–19677, https://doi.org/10.1021/acs.jpcc.6b04957.
[12] X. Lu, M. Mohedano, C. Blawert, E. Matykina, R. Arrabal, K.U. Kainer, M. L. Zheludkevich, Plasma electrolytic oxidation coatings with particle additions – a review, Surf. Coat. Technol. 307 (2016) 1165–1182, https://doi.org/10.1016/j.surfcoat.2016.08.055.
[13] J.S. Gandhi, S. Singh, W.J. Van Ooij, P. Puomi, Evidence for formation of metallo-siloxane bonds by comparison of dip-coated and electrodeposited silane films, J. Adhes. Sci. Technol. 20 (2006) 1741–1768, https://doi.org/10.1163/156856106779024481.
[14] A. Nazarov, A.P. Romano, M. Fedel, F. Deflorian, D. Thierry, M.G. Olivier, Filiform corrosion of electrocoated aluminium alloy: role of surface pretreatment, Corros. Sci. 65 (2012) 187–198, https://doi.org/10.1016/j.corsci.2012.08.013.
[15] F. Cavezza, M. Boehm, H. Terryn, T. Hauffman, A review on adhesively bonded aluminium joints in the automotive industry, Metals 10 (2020) 1–32, https://doi.org/10.3390/met10060730.
[16] F. Cavezza, M. Boehm, H. Terryn, T. Hauffman, A review on adhesively bonded aluminium joints in the automotive industry, Metals 10 (2020), https://doi.org/10.3390/met10060730.
[17] J.B. Bajat, O. Dedić, Adhesion and corrosion resistance of epoxy primers used in the automotive industry, J. Adhes. Sci. Technol. 21 (2007) 819–831, https://doi.org/10.1163/156856107781061512.
[18] Š. Sedonja, J.F. Watts, M. Oldfield, A. Sordon, G. Örn Gunnarsson, A. Viquerat, The adhesion of aluminium inserts in epoxy composites: the role of surface pre-treatment, Int. J. Adhes. Adhes. 118 (2022), https://doi.org/10.1016/j.ijadhadh.2022.103196.
[19] N. Parhizkar, B. Ramezanzadeh, T. Shahrabi, Corrosion protection and adhesion properties of the epoxy coating applied on the steel substrate pre-treated by a sol-gel based silane coating filled with amino and isocyanate silane functionalized graphene oxide nanosheets, Appl. Surf. Sci. 439 (2018) 45–59, https://doi.org/10.1016/j.apsusc.2017.12.240.
[20] M. Doerre, L. Hibbitts, G. Patrick, N.K. Akafuah, Advances in automotive conversion coatings during pretreatment of the body structure: a review, Coatings 8 (2018), https://doi.org/10.3390/coatings8110405.
[21] S. Sharifi Golru, M.M. Attar, B. Ramezanzadeh, Effects of surface treatment of aluminium alloy 1050 on the adhesion and anticorrosion properties of the epoxy coating, Appl. Surf. Sci. 345 (2015) 360–368, https://doi.org/10.1016/j.apsusc.2015.03.148.
[22] J.B. Bajat, O. Dedic, Adhesion and corrosion resistance of epoxy primers used in the automotive industry, 21:9, 819-831, (2007), doi:10.1163/156856107781061512.

[23] A. Trentin, S.V. Harb, M.C. Uvida, K. Marcoen, S.H. Pulcinelli, C.V. Santilli, H. Terryn, T. Hauffman, P. Hammer, Effect of Ce(III) and Ce(IV) ions on the structure and active protection of PMMA-silica coatings on AA7075 alloy, Corros. Sci. 189 (2021) 109581, https://doi.org/10.1016/j.corsci.2021.109581.
[24] G.D. Sulka, W.J. Stepniowski, Structural features of self-organized nanopore arrays formed by anodization of aluminum in oxalic acid at relatively high temperatures, Electrochim. Acta 54 (2009) 3683–3691, https://doi.org/10.1016/j.electacta.2009.01.046.
[25] K.Y. Huang, C.J. Weng, S.Y. Lin, Y.H. Yu, J.M. Yeh, Preparation and anticorrosive properties of hybrid coatings based on epoxy-silica hybrid materials, J. Appl. Polym. Sci. 112 (2009) 1933–1942, https://doi.org/10.1002/app.29302.
[26] K. Pohl, O. Ozcan, M. Voigt, G. Grundmeier, Adhesion and corrosive delamination of epoxy films on chemically etched ZnMgAl-alloy coatings, Mater. Corros. 67 (2016) 1020–1026, https://doi.org/10.1002/maco.201608968.
[27] S.T. Abrahami, J.M.M. de Kok, V.C. Gudla, R. Ambat, H. Terryn, J.M.C. Mol, Interface strength and degradation of adhesively bonded porous aluminum oxides, Npj Mater Degrad (2017) 1, https://doi.org/10.1038/s41529-017-0007-0.
[28] O. Hara, Curing agents for epoxy resin, Tokyo, 1990. https://www.threebond.co.jp/en/technical/technicalnews/pdf/tech32.pdf (accessed September 26, 2023).
[29] G. Cruz-Quesada, M. Espinal-Viguri, M.V. López-Ramón, J.J. Garrido, Hybrid xerogels: study of the sol-gel process and local structure by vibrational spectroscopy, Polymers 13 (2021), https://doi.org/10.3390/polym13132082.
[30] M. González González, J.C. Cabanelas, J. Baselga, Applications of FTIR on epoxy resins-identification, monitoring the curing process, phase separation and water uptake, in: T. Theophanides (Ed.), Infrared Spectroscopy – Materials Science, Engineering and Technology, InTech, 2012, pp. 261–284, https://doi.org/10.5772/36323.
[31] B.L. Denq, Y.S. Hu, L.W. Chen, W.Y. Chiu, T.R. Wu, The curing reaction and physical properties of DGEBA/DETA epoxy resin blended with propyl ester phosphazene, J. Appl. Polym. Sci. 74 (1999) 229–237, https://doi.org/10.1002/(SICI)1097-4628(19991003)74:1<229::AID-APP28>3.0.CO;2-C.
[32] G. Nikolic, S. Zlatkovic, M. Cakic, S. Cakic, C. Lacnjevac, Z. Rajic, Fast fourier transform IR characterization of epoxy GY systems crosslinked with aliphatic and cycloaliphatic EH polyamine adducts, Sensors 10 (2010) 684–696, https://doi.org/10.3390/s100100684.
[33] M.C. Uvida, P. Hammer, A.D.A. Almeida, S.H. Pulcinelli, C.V. Santilli, Structural properties of epoxy-silica barrier coatings for corrosion protection of reinforcing steel, Polymers 14 (2022) 3474, https://doi.org/10.3390/polym14173474.
[34] M.C. Uvida, A. Trentin, S.V. Harb, S.H. Pulcinelli, C.V. Santilli, P. Hammer, Nanostructured poly(methyl methacrylate)−silica coatings for corrosion protection of reinforcing steel, ACS Appl. Nano Mater. 5 (2022) 2603–2615, https://doi.org/10.1021/acsanm.1c04281.
[35] F.C. Dos Santos, S.V. Harb, M.J.. Menu, V. Turq, S.H. Pulcinelli, C.V. Santilli, P. Hammer, On the structure of high performance anticorrosive PMMA–siloxane-silica hybrid coatings, RSC Adv 5 (2015) 106754, https://doi.org/10.1039/C5RA20885H.
[36] R.F.A.O. Torrico, S.V. Harb, A. Trentin, M.C. Uvida, S.H. Pulcinelli, C.V. Santilli, P. Hammer, Structure and properties of epoxy-siloxane-silica nanocomposite coatings for corrosion protection, J. Colloid Interface Sci. 513 (2018) 617–628, https://doi.org/10.1016/j.jcis.2017.11.069.
[37] Z. Feng, G.S. Frankel, Evaluation of coated Al alloy using the breakpoint frequency method, Electrochim. Acta 187 (2016) 605–615, https://doi.org/10.1016/j.electacta.2015.11.114.
[38] A. Trentin, A. Pakseresht, A. Duran, Y. Castro, D. Galusek, Electrochemical characterization of polymeric coatings for corrosion protection : a review of advances and perspectives, Polymers 14 (2022) 2306, https://doi.org/10.3390/polym14122306.
[39] L. Philippe, C. Sammon, S.B. Lyon, J. Yarwood, An FTIR/ATR in situ study of sorption and transport in corrosion protective organic coatings 1. Water sorption and the role of inhibitor anions, Prog. Org. Coat. 49 (2004) 302–314, https://doi.org/10.1016/j.porgcoat.2003.07.002.
[40] S. Akbarzadeh, M. Ramezanzadeh, B. Ramezanzadeh, Inspection the corrosion prevention performance and dry/wet interfacial adhesion qualities of the melamine-cured polyester coating applied on the treated mild steel surface with a nanostructured composite cerium-neodymium film, Colloids Surf. A Physicochem. Eng. Asp 590 (2020), https://doi.org/10.1016/j.colsurfa.2020.124472.
[41] A.H.J. Mofidabadi, G. Bahlakeh, B. Ramezanzadeh, Explorations of the adhesion and anti-corrosion properties of the epoxy coating on the carbon steel surface modified by Eu2O3 nanostructured film, J. Mol. Liq. 314 (2020), https://doi.org/10.1016/j.molliq.2020.113658.
[42] J. Wielant, T. Hauffman, O. Blajiev, R. Hausbrand, H. Terryn, Influence of the iron oxide acid-base properties on the chemisorption of model epoxy compounds studied by XPS, J. Phys. Chem. C 111 (2007) 13177–13184, https://doi.org/10.1021/jp072354j.